Optical transmission through double-layer, laterally shifted metallic subwavelength hole arrays

Z. Marcet,[1] Z. H. Hang,[2] C. T. Chan,[2] I. Kravchenko,[3] J. E. Bower,[4] R. A. Cirelli,[4] F. Klemens,[4] W. M. Mansfield,[4] J. F. Miner,[4] C. S. Pai,[4] and H. B. Chan[1,2,*]

[1]*Department of Physics, University of Florida, Gainesville, Florida 32611, USA*

[2]*Department of Physics, The Hong Kong University of Science and Technology, Clear Water Bay, Kowloon, Hong Kong, China*

[3]*Center for Nanophase Materials Sciences, Oak Ridge National Laboratory, Oak Ridge, Tennessee 37830, USA*

[4]*Bell Laboratories, Alcatel-Lucent, Murray Hill, New Jersey 07974, USA*

**Corresponding author: hochan@ust.hk*

Received February 11, 2010; revised April 30, 2010; accepted May 17, 2010;
posted June 7, 2010 (Doc. ID 124083); published June 16, 2010

We measure the transmission of IR radiation through double-layer metal films with periodic arrays of subwavelength holes. When the two metal films are placed in sufficiently close proximity, two types of transmission resonances emerge. For the surface plasmon mode, the electromagnetic field is concentrated on the outer surface of the entire metallic layer stack. In contrast, for the guided mode, the field is confined to the gap between the two metal layers. Our measurements indicate that, as the two layers are laterally shifted from perfect alignment, the peak transmission frequency of the guided mode decreases significantly, while that of the surface plasmon mode remains largely unchanged, in agreement with numerical calculations. © 2010 Optical Society of America

OCIS codes: 050.2770, 240.6680, 240.6690, 310.4165, 310.6628, 310.6860.

Subwavelength features on metallic layers enable the resonant excitation of surface waves by incident electromagnetic radiation, leading to remarkable properties, such as extraordinarily high transmission [1] and beaming capabilities [2]. By placing two such metallic layers in close proximity, it is possible to control the coupling of the strong evanescent fields to achieve novel optical characteristics that are absent in single layers [3–17]. For instance, double-layer fishnet structures have been demonstrated to exhibit negative refraction in the mean field regime [18–22]. Another example involves double-layer slit arrays that enable the phase delay of the transmitted radiation to be controlled through lateral displacement between the two layers [23]. It is also well known that multiple solid metal layers support guided modes that propagate parallel to the surfaces in the air gap between them [24]. The presence of subwavelength features could allow the coupling of these guided modes to incident radiation.

Despite recent progress, the vast majority of optical transmission measurements involve bilayer subwavelength structures in which the two layers are perfectly aligned [4,9,14,18,20]. In this letter, we report measurements of the optical transmission through bilayer subwavelength hole arrays with different lateral shifts between the two layers. By comparing to calculations, we identified two mechanisms of strong transmission at different wavelengths: The first mode is associated with strong evanescent fields at the incident and exit surfaces, resembling the field distribution of a single layer at resonance. Maximum transmission occurs at a wavelength that is largely independent of the lateral shift between the two metal layers. For the second mode, in contrast, the local field is concentrated in the gap between the two metal layers. This mode has no analogue in single-layer structures. The wavelength at which maximum transmission occurs depends strongly on the lateral shift between the two metal layers.

Our samples consist of single- and double-layer aluminum films patterned with a two-dimensional square array of subwavelength holes [Fig. 1(a)] on a quartz substrate. Each metallic layer is 0.39 μm thick. Hole arrays with x and y periodicity of 1 μm are created by lithographically patterning a photoresist layer, followed by reactive ion etching into the aluminum. The circular openings have slightly slanted sidewalls, so that their diameter is reduced from 0.5 μm on the top surface to 0.42 μm on the bottom surface. Sample A consists of a hole array on a single layer of aluminum. In the double-layer samples (B1 and B2), the metal films are separated by 0.3 μm

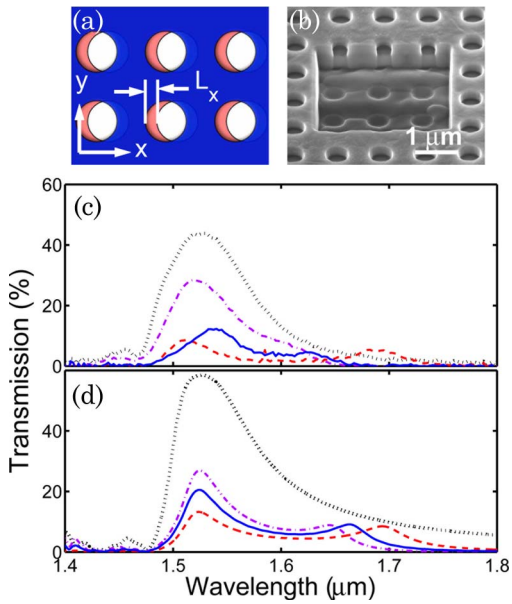

Fig. 1. (Color online) (a) Structure of the double-hole array. (b) Part of the top metal layer and the oxide spacer is removed by focus ion beam to reveal the bottom hole array. (c) Measured optical transmission of samples A (dotted curve), B1 (dashed–dotted curve), and B2 (solid curve) for incident $\vec{E}$ polarized in the x direction. The dashed curve represents the transmission through sample B2 with $\vec{E}$ in the y direction. (d) Transmission calculated with finite-difference time-domain (FDTD).

to allow coupling of the evanescent fields on the two layers. The metal layers in both the single- and double-layer structures are completely surrounded by silicon oxide. As illustrated in Fig. 1(a), the two hole arrays in the double-layer samples are laterally shifted in the x direction by distance L, ranging from 0 to 0.5 μm (half the array period). Figure 1(b) is a scanning electron micrograph on a sample without the top insulating oxide layer so that the hole array can be visualized.

We measured the transmission of linearly polarized light through our samples using a Fourier transform IR spectrometer. All transmission spectra have been normalized by using the measured transmission through a clear region adjacent to the subwavelength structures, consisting of the quartz wafer and a layer of silicon oxide. To identify and distinguish the different mechanisms for transmission through the structures, we compared our measurements to FDTD simulations (Concerto 6.5 by Vector Field, Inc.). The exact experimental configurations, including the plate thickness, size, and shape of the apertures and properties of background materials, were used in the simulations and the relative permittivity of aluminum is modeled by the Drude model, whose parameters are determined from the infrared optical constant of aluminum [25].

Figures 1(c) and 1(d) show, respectively, the measured and calculated transmission spectra of our structures at wavelengths much larger than the hole diameter. The dotted curve in Fig. 1(c) shows the measured transmission through the single-layer hole array (sample A) with the electric field $\vec{E}$ of the incident light polarized in the x direction. Even though the fractional area of the holes is less than 15%, the peak transmission at a wavelength of 1.53 μm reaches about 50%. Taking into account the refractive index of the silicon oxide (1.47) surrounding the structures, the peak transmission occurs at a wavelength slightly higher than the 1 μm periodicity of the holes. This transmission peak has been extensively studied, and its origin has been attributed to the excitation of surface plasmons [1] or diffracted evanescent waves [26]. Comparison of the measured single-layer transmission to calculations in Fig. 1(d) indicates good agreement in both the peak position and the transmission magnitude.

Next, we study the transmission properties of double-layer hole arrays. We fabricated a set of samples with different lateral shifts L between the hole arrays in the two layers, ranging from 0 (perfect alignment) to 0.5 μm (half the period) in the x direction. The dashed–dotted curve in Fig. 1(c) shows the transmission of linearly polarized light with $\vec{E}$ in the x direction through sample B1 with $L = 0$. Comparing the measurement results to FDTD calculations reveals the existence of two transmission peaks, one at 1.53 μm with transmission of 30%, and another at 1.6 μm with transmission of about 10%. As explained later, we identify the former as the surface plasmon (SP) mode and the latter as the guided mode. The guided mode peak is barely visible in measurements due to additional losses from sample inhomogeneity but is well resolved in calculations. For sample B2, with $L = 0.5$ μm, the two peaks are clearly distinguishable in the measured transmission curves, as shown in Fig. 1(c) by the solid curve and the dashed curve for $\vec{E}$ of the incident light along the x and y directions, respectively. Comparing the measurement results to FDTD calculations in Fig. 1(d) gives good agreement. An important difference between the SP mode and the guided mode is that, as the lateral shift between the two layers increases, the wavelength of the former remains largely unchanged, while the guided mode peak shifts to longer wavelengths.

The different behaviors of the SP mode and the guided mode can be understood by examining the electromagnetic field distributions obtained from the FDTD simulations. Figure 2(a) shows the z component of the electric field distribution E_z for the aligned sample B1, for the SP mode with the incident electric field along the x direction and the magnetic field along the y direction. The regions with strong E_z field are associated with large surface charge densities. Strong surface electromagnetic fields are present on the outer surfaces of the double layer, with a field distribution similar to that on the two surfaces of a single-layer structure. As the total double-layer structure is thick, the surface wave has a lower intensity on the exit surface than that on the incident surface. When the hole array in the two layers are laterally offset by 0.5 μm (half the periodicity), the fields remain concentrated on the outer surfaces and are essentially the same, as shown in Fig. 2(b). The resonance wavelength is almost unchanged by the lateral shift.

For the guided mode, the field distribution depends strongly on the lateral shift. Figure 2(c) shows that, in the aligned sample B1, E_z on the outer surface is significantly weaker. Instead, the surface charge is confined to the gap between the two metallic layers. We refer to this resonance as the guided mode because the propagation of the field inside the gap is along the gap in a direction orthogonal to the incident light [24], just like the transverse electromagnetic mode existing between two metallic plates in proximity. In the literature, this mode has also been called a gap SP or internal SP [16,21]. The hole arrays on the metal plates enable the guided mode to be coupled to incident light of appropriate wavelength, giving rise to the transmission maximum. When the two hole arrays are misaligned, the mode profiles are

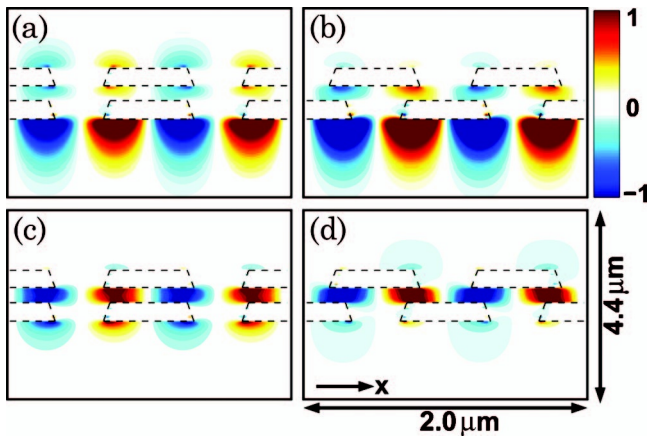

Fig. 2. Longitudinal E_z field distribution for (a) the SP mode of sample B1, (b) the SP mode of sample B2, (c) the guided mode of sample B1, and (d) the guided mode of sample B2. The incoming wave is polarized along the x direction from the bottom with unit amplitude. Field with intensity exceeding unit amplitude is plotted in the same color as unit amplitude. The dashed lines enclose the metallic region.

changed, leading to a shift of the resonant wavelength of the guided mode.

Recently, the optical transmission through double-layer slit arrays has also been investigated [11,23]. Like subwavelength hole arrays, SP resonance is found to play an important role. The main difference is that individual slits with sufficient thickness support propagating waveguide modes, whereas such modes are evanescent in subwavelength holes. As a result, the optical properties of single- and double-layer slit arrays are qualitatively different from hole arrays. In particular, calculations indicate that the guided mode observed here in double-layer hole arrays are absent in double-layer slit arrays, consistent with previous experiments [11,23].

Our results demonstrate that the relative lateral displacement could have a strong influence on the optical properties of multilayer subwavelength metallic structures. Apart from the effect on the resonant wavelength of various transmission modes shown here, it appears likely that lateral shift of the two metal layers could also modify the time delay of optical pulses transmitted through the structure. With the proper design, bilayer hole arrays have been shown to exhibit negative refraction at specific wavelengths [18–22]. The effect of the lateral shift on negative refraction is an interesting topic that warrants further investigation.

Z. M. and H. B. C. are supported by the National Science Foundation (NSF) ECS-0621944. Z. M. acknowledges support from South East Alliance for Graduate Education and the Professoriate. Z. H. H. and C. T. C. are supported by Hong Kong Research Grants Council (RGC) grant 600308. A portion of this research was conducted at the Center for Nanophase Materials Sciences, which is sponsored at Oak Ridge National Laboratory by the Division of Scientific User Facilities, U.S. Department of Energy. We thank J. D. Fowlkes and G. Suen for assistance with the focus ion beam.

References

1. T. W. Ebbesen, H. J. Lezec, H. F. Ghaemi, T. Thio, and P. A. Wolff, Nature **391**, 667 (1998).
2. H. J. Lezec, A. Degiron, E. Devaux, R. A. Linke, L. Martin-Moreno, F. J. Garcia-Vidal, and T. W. Ebbesen, Science **297**, 820 (2002).
3. Z. N. Yu, P. Deshpande, W. Wu, J. Wang, and S. Y. Chou, Appl. Phys. Lett. **77**, 927 (2000).
4. R. M. Bakker, V. P. Drachev, H.-K. Yuan, and V. M. Shalaev, Opt. Express **12**, 3701 (2004).
5. D. Gérard, L. Salomon, F. de Fornel, and A. V. Zayats, Phys. Rev. B **69**, 113405 (2004).
6. A. P. Hibbins, J. R. Sambles, C. R. Lawrence, and J. R. Brown, Phys. Rev. Lett. **92**, 143904 (2004).
7. J. T. Shen and P. M. Platzman, Phys. Rev. B **70**, 035101 (2004).
8. F. Miyamaru and M. Hangyo, Phys. Rev. B **71**, 165408 (2005).
9. J. H. Ye and J. Y. Zhang, Opt. Lett. **30**, 1521 (2005).
10. Q. Li, X. Jiao, P. Wang, H. Ming, and J. Xie, Appl. Phys. B **81**, 787 (2005).
11. H. B. Chan, Z. Marcet, K. Woo, D. B. Tanner, D. W. Carr, J. E. Bower, R. A. Cirelli, E. Ferry, F. Klemens, J. Miner, C. S. Pai, and J. A. Taylor, Opt. Lett. **31**, 516 (2006).
12. C. Cheng, J. Chen, Q.-Y. Wu, F.-F. Ren, J. Xu, Y.-X. Fan, and H.-T. Wang, Appl. Phys. Lett. **91**, 111111 (2007).
13. X. Fang, Z. Li, Y. Long, H. Wei, R. Liu, J. Ma, M. Kamran, H. Zhao, X. Han, B. Zhao, and X. Qiu, Phys. Rev. Lett. **99**, 066805 (2007).
14. Z. H. Tang, R. W. Peng, Z. Wang, X. Wu, Y. J. Bao, Q. J. Wang, Z. J. Zhang, W. H. Sun, and M. Wang, Phys. Rev. B **76**, 195405 (2007).
15. M.-D. He, L.-L. Wang, J.-Q. Liu, X. Zhai, Q. Wan, X. Chen, and B. S. Zou, Appl. Phys. Lett. **93**, 221909 (2008).
16. R. Ortuno, C. García-Meca, F. J. Rodríguez-Fortuno, J. Martí, and A. Martínez, Phys. Rev. B **79**, 075425 (2009).
17. C. H. Gan and G. Gbur, Opt. Express **17**, 20553 (2009).
18. S. Zhang, W. Fan, N. C. Panoiu, K. J. Malloy, R. M. Osgood, and S. R. J. Brueck, Phys. Rev. Lett. **95**, 137404 (2005).
19. M. Beruete, M. Sorolla, M. Navarro-Cía, F. Falcone, I. Campillo, and V. Lomakin, Opt. Express **15**, 1107 (2007).
20. Z. Ku and S. R. J. Brueck, Opt. Express **15**, 4515 (2007).
21. A. Mary, S. G. Rodrigo, F. J. Garcia-Vidal, and L. Martin-Moreno, Phys. Rev. Lett. **101**, 103902 (2008).
22. C. García-Meca, R. Ortuno, F. J. Rodríguez-Fortuno, J. Martí, and A. Martínez, Opt. Lett. **34**, 1603 (2009).
23. Z. Marcet, J. W. Paster, D. W. Carr, J. E. Bower, R. A. Cirelli, F. Klemens, W. M. Mansfield, J. F. Miner, C. S. Pai, and H. B. Chan, Opt. Lett. **33**, 1410 (2008).
24. E. N. Economou, Phys. Rev. **182**, 539 (1969).
25. E. D. Palik, ed., *Handbook of Optical Constants of Solids* (Academic, 1985).
26. H. J. Lezec and T. Thio, Opt. Express **12**, 3629 (2004).